

Chitosan-templated Cu₂O Aerogel for Efficient Iodine Capture

Renren Wang^{1,2}, Yi Tan^{1,2}, Mengling Huang^{1,2}, Guangyuan Cheng^{1,2}, Qian Zhao^{1,2}, Jian Liu^{1,2}, Pengwei Meng^{1,2}, Lin Zhu^{1,2}, Yongjian Tang^{1,2}, Tao Duan^{1,2,*}

¹ National Co-Innovation Center for Nuclear Waste Disposal and Environmental Safety, Southwest University of Science and Technology, Mianyang 621010, China

² Fundamental Science on Nuclear Wastes and Environmental Safety Laboratory, Southwest University of Science and Technology, Mianyang 621010, China

*Correspondence: duant@ustc.edu.cn

Abstract

Developing a series of efficient adsorbents is very important for the separation of radioactive iodine during the spent fuel reprocessing. In this work, cuprous oxide aerogel material was successfully prepared by sol-gel method with the template of chitosan. The template was removed by calcination, through comparative experiments, the optimal calcination temperature was 600 °C and the calcination time was 200 min. Through the characterization analysis of XRD, SEM, FTIR and BET, the results show that cuprous oxide aerogels exhibit a 3-dimensional porous structure by linking with nanorods, with the specific surface area of 2.1 m²/g and the pore size distribution of 3-18 nm. The sorption experiments of iodine on Cu₂O aerogel were systematically investigated. Through the batch adsorption experiment, the maximum adsorption capacity of iodine on Cu₂O aerogel is 636.7 mg/g, and the adsorption mechanism was unraveled by XRD and FTIR, where iodine binds to Cu₂O aerogel forming Cu-I bonds, belongs to the chemical adsorption process. Through thermal and acid-base stability experiments, we also prove that Cu₂O aerogel has good thermal and chemical stability, which may be considered as an efficient iodine adsorbent for iodine capture.

Keywords

Cuprous Oxide; Aerogel; Sorption; Iodine.

1. Introduction

With the rapid development of population and economy, the rapid growth of world energy demand, the non-renewable nature of traditional fossil energy and greenhouse gas emissions, the crisis of energy depletion and ecological environment is becoming more and more serious[1,2]. As a kind of future energy, nuclear energy has the advantages of high energy density, no greenhouse gas emissions, safety and reliability, and is regarded as the most promising solution to solve the double crisis of human energy and environment[3]. In recent years, nuclear energy has attracted more and more attention by governments, the world has entered a new round of nuclear power construction, the proportion of nuclear power in the international energy pattern has been steadily increasing, the scale of nuclear power in China is also increasing rapidly, and the nuclear power generation has exceeded 5% of the total power generation in 2020[4,5].

But nuclear power plants can produce large amounts of radioactive waste during their operation, including a large number of radioactive gases (3H, 14C, 129I, 131I, 85Kr, 133Xe, etc.)[6], for instance, when the UO_x spent fuel is dissolved in a boiling nitric acid solution, most of the CsI is oxidized to a volatile radioactive I₂ (129I, 131I) escaping from the solution, since radioactive iodine

(mainly ^{129}I) has a very long half-life (15.7 million years)[7-9], and it is easy to combine with surface water and groundwater and rapid migration resulting in a large range of radioactive pollution[10]. In particular, once the radioactive iodine is ingested by the human body through the biological chain and the food chain, will seriously disrupt the body's metabolism and the development of brain intelligence, even leading to a significantly higher risk of developing thyroid tumors[11,12]. For example, after the Chernobyl and Fukushima nuclear accidents, a large amount of radioactive iodine (mainly ^{131}I and ^{129}I) entered the environment and quickly spread to a considerable range of surrounding land, sea and atmosphere, causing serious radiation pollution[13]. Therefore, how to efficiently remove gaseous radioactive iodine in spent fuel treatment has become one of the key preconditions for the safe operation of nuclear power plants.

Radioactive iodine (mainly in ^{129}I) is usually present in the form of iodine alone, or possibly a single or multiple anionic substances (i. e., iodine ion (I^-), iodide ion (IO_3^-))[14]. At present, the emitted iodine in the removal of spent fuel mainly includes liquid phase washing method and solid phase adsorption method[15]. Because the liquid phase washing method is complicated, expensive and causes secondary pollution, the removal of iodine in spent fuel treatment[16]. And solid phase adsorption method is simple, high removal efficiency, no secondary pollution and other obvious comparative advantages[17], so the pretreatment process mainly adopts solid phase adsorption method to remove gaseous radioactive iodine, common adsorption of iodine solid phase adsorbent materials including silver zeolite[18], activated carbon[19], metal organic skeleton materials (MOFs)[20], covalent organic frame compounds (COFs)[21], porous organic polymer (POPs)[22] and aerogel materials[24-26] etc. The aerogel material with extensive material source, simple preparation, adsorption can directly sintering after curing and quickly become a popular iodine adsorbent material[23], has been reported successful synthesis of silver-based aerogel[24], sulfur-based aerogel[25], bismuth-based aerogel[26] and other types of aerogel for iodine showed high capture performance. On the basis of these studies, we propose a synthesis method of cuprous oxide aerogel, and study the adsorption behavior of iodine, effectively exploring the transition metal aerogel material for iodine removal.

2. Experiment

2.1 Material Preparation

Reagents: Deionized water, copper sulfate (CuSO_4 , $\geq 99\%$), polyvinylpyrrolidone ($(\text{C}_6\text{H}_9\text{NO})_n$, $\geq 99\%$), trisodium citrate ($\text{C}_6\text{H}_5\text{Na}_3\text{O}_7$), anhydrous sodium carbonate (Na_2CO_3 , $\geq 99.9\%$), glucose ($\text{C}_6\text{H}_{12}\text{O}_6$), chitosan ($(\text{C}_6\text{H}_{11}\text{NO}_4)_n$, $\geq 99\%$), hydrochloric acid (HCl , 5%), iodine (I_2 , $\geq 99.9\%$), cyclohexane (C_6H_{12} , $\geq 99\%$) were purchased from Aladdin Chemistry Co. Ltd. (China). All chemicals used in this study were of analytical grade and used without further purification.

Instruments: Electronic balance (BSA-124s, Beijing Sartorius Scientific Instrument Co., LTD.), vacuum drying box (DZF-6050, Shanghai Yiheng Technology Co., LTD.), Maver furnace (HR-F1200, Luoyang Huarong Kiln Co., Ltd), scanning electron microscope (SEM) (EVO 18, German Zeiss), specific surface area and porosity analyzer (BET) (II 3020, US. Mcromeritics Tristar), X-ray powder diffractor (XRD) (TD-3500X, Dutch, Panalytical Co., LTD.), Fourier transform infrared absorption spectrum (FTIR) (UV1000, Techcomp (China) Scientific Instruments Co., LTD), ultraviolet spectrophotometer (UV26002, Uniico (Shanghai) Instrument Co., LTD.).

Preparation of Cu_2O aerogel : Stirring 108.5 mg CuSO_4 and 15 mg PVP (polyvinylpyrrolidone) in 1 mL of deionized water, add 191 mg of sodium citric rate, 148.4 mg anhydrous sodium carbonate and 1 mL deionized water and stir well, add 1 mL of glucose solution (27.74wt%) and 10 mL of glucose solution and 10 mL of chitosan solution (10 mL of HNO_3 (5wt%), 0.15g of chitosan) for 30 min to obtain the blue mixture, The resulting mixture was then stirred and heated in an 80 °C oil bath for 2h, sonicated for 30 min, and freeze-dried for 72 h, The last 600 °C was calcined for 200 min, To get the cuprous oxide aerogels, The appearance is a dark-brown, pink-shaped solid.

2.2 Batch Adsorption Experiment

In this experiment, 99.9% purity of iodine as iodine source and cyclohexane as solvent to prepare iodine solution. Iodine solution adsorption: a certain quality of adsorbent material is added to a certain volume of iodocyclohexane solution, after the adsorption is completed, the solution is filtered, and then the concentration of iodine in the filtrate is measured with an ultraviolet spectrophotometer. Establish standard curve: a series of concentration gradient iodocyclohexane solutions, the absorbance was measured by UV spectrophotometer, and a standard curve of iodine-cyclohexane was established ($R^2 > 0.999$) (Figure 1).

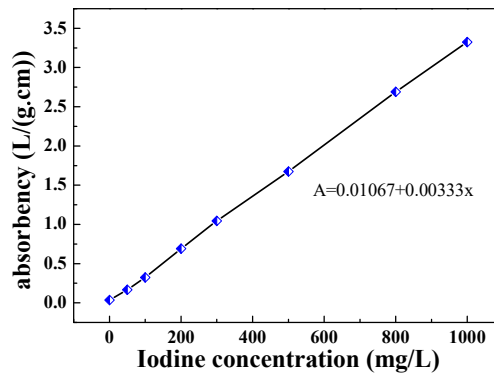


Figure 1. Absorbency curve of the iodine-cyclohexane solution

2.3 Data Analyse

The adsorption amount of iodine of the material is calculated by formula (1); C_0 (mg/L) and C_e (mg/L) represent the concentration of iodine before and after adsorption, v (L) is the initial volume of the solution and M (mg) is the mass of the adsorbent.

$$q_e = \frac{(C_0 - C_e)V}{M} \quad (1)$$

The adsorption isothermal curve is fitted according to Langmuir equation (2) and Freundlich equation (3). The concentration of iodine solution is ρ_e , unit mg/L; q_e and q_{\max} is the adsorption amount and maximum amount of adsorbed material respectively, unit mg/g; b and K_f are constants related to the adsorption energy, and n is constant.

$$\frac{\rho_e}{q_e} = \frac{\rho_e}{q_{\max}} + \frac{1}{bq_{\max}} \quad (2)$$

$$\ln q_e = \ln K_f + n \ln c_e \quad (3)$$

The adsorption kinetic curve is fitted by the pseudo-first-order kinetic equation (4) and the pseudo-second-order kinetic equation (5), where q_t and q_e represent the I2 adsorption at time t and equilibrium, mg/g; k_1 and k_2 represent the adsorption rate constants of both equations in min^{-1} and $\text{g}/(\text{mg} \cdot \text{min})$; t is the adsorption time.

$$\ln(q_e - q_t) = \ln q_e - K_1 t \quad (4)$$

$$\frac{t}{q_t} = \frac{1}{k_2 \times q_e^2} + \frac{t}{q_e} \quad (5)$$

3. Results and Discussion

3.1 Material Characterization

This study using German Zeiss EVO 18 high resolution cold field emission scanning microscope to characterize the cuprous oxide aerogel material as shown in Figure 2(c)(d), (c) figure is 3-D mesh structure is a typical aerogel microstructure features, proved that the experiment successfully synthesized the expected cuprous oxide aerogel material, (d) local details show the 3-D mesh structure of cuprous oxide nanoparticles accumulation.

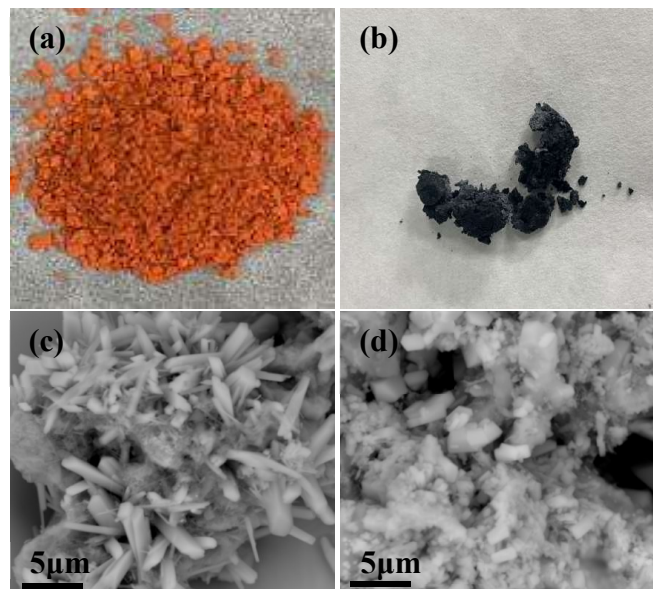


Figure 2. (a)(b) Optical photos of the Cu₂O aerogel before and after adsorption of iodine; (c)(d) SEM images of the Cu₂O aerogel

Figure 3 (a)(b) shows XRD spectra before and after iodine adsorption on Cu₂O aerogel. As shown in Figure (a), Cu₂O peaks appear at $2\theta = 26.69, 36.52$ and 42.41 , indicating the Cu₂O aerogel material was successfully synthesised[27]; After iodine sorption, Figure (b) shows that the structure changes and the crystallinity is significantly reduced into amorphous structure and a new peak ascribed to CuI can be found at 25.5° [28].

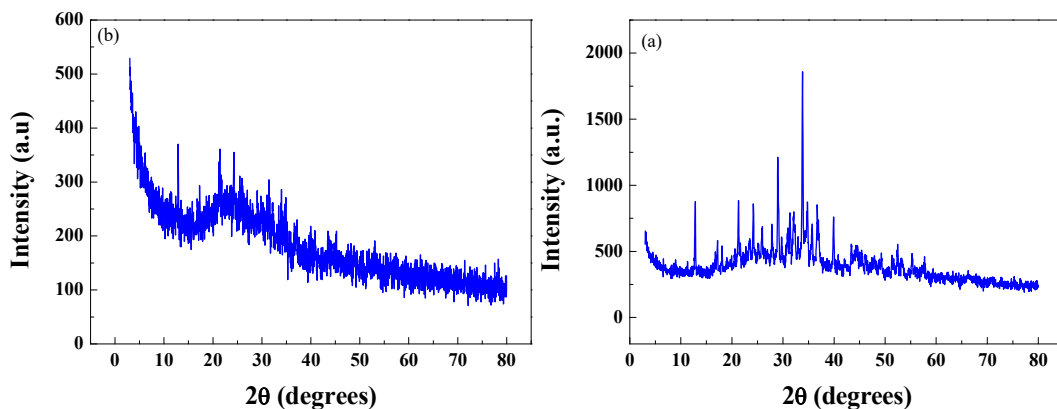


Figure 3. XRD patterns of Cu₂O aerogel (a) before and (b) after iodine adsorption

From the comparative literature in the data before and after Cu₂O aerogel adsorption in Figure 4, O-H tensile vibration was detected at 3450 cm⁻¹ [29], the band detected at 620 cm⁻¹ is Cu-O bonds in Cu₂O, and the other two peaks at 3426 cm⁻¹ and 1603 cm⁻¹ are respectively due to tensile and bending vibrations due to Cu₂O surface due to hydroxyl group. The observed at 2350 cm⁻¹ reflects the expansion vibration of impurities in the nanocomposite [30,31].

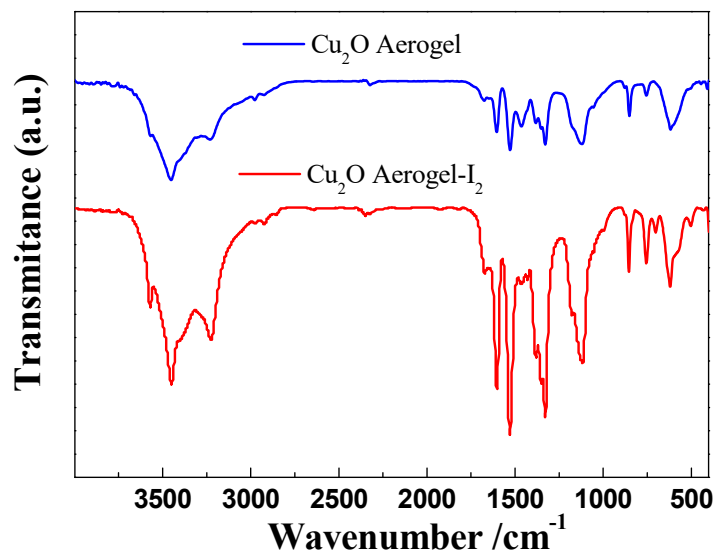


Figure 4. FTIR images before and after iodine adsorption on the Cu₂O aerogel

Figure 5 shows the analysis diagram of nitrogen adsorption of Cu₂O aerogel. When the relative pressure (p/p_0) is in the range of 0-0.9, the adsorption and desorption of N₂ are positively correlated with the relative pressure value (shown in Figure 5(a)), the adsorption of nitrogen molecules is surface monolayer. When the adsorption pressure reaches 0.9, it may be related to the formation of capillary condensation by nitrogen molecule micropores inside the copper oxide aerogel. In Figure 5(b), the pore diameter of the three-dimensional mesh structure of copper oxide aerogel is mainly distributed in 3-18 nm, and the average pore diameter is about 6 nm, and the specific surface area is 2.1 m²/g. In conclusion, this chapter has successfully synthesized aerogous oxide aerogel material, which has Cu₂O nanorods accumulation into three-dimensional mesh structure, large specific surface area and uniform pore size distribution, has certain advantages in adsorption and separation, and can be used as an iodine adsorbent material.

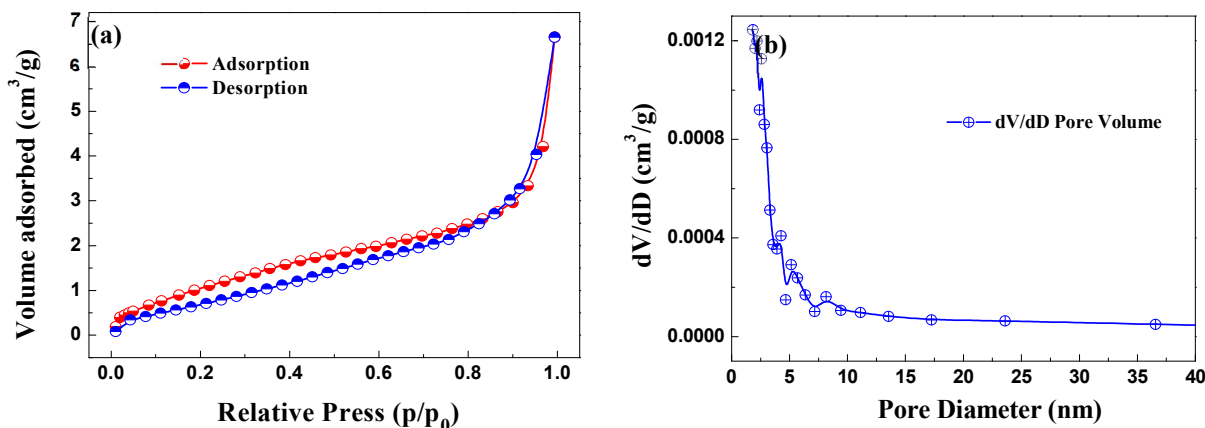


Figure 5. The BET curves of the Cu₂O aerogel material

3.2 Adsorption Kinetics

Put excessive iodine into a small brown glass bottle, put 200 mg of copper oxide aerogel on the top of the lid at the top of the bottle, and heat the device to 75°C under ambient pressure. After a certain time, the sample was cooled to room temperature and weighed to calculate iodine capture, and four parallel experiments were performed. The iodine adsorption capacity of bismuth aerogel pair is calculated according to formula (6). In formula (6), Q (mg/g) is the adsorption capacity of iodine, and m_1 and m_2 are the quality of bismuth aerogel before and after capturing iodine.

$$Q = \frac{(m_2 - m_1)}{m_1} \times 100 \text{ wt\%} \quad (6)$$

The kinetic curve of iodine adsorption of copper oxide aerogel at 75°C is shown in Figure 6, when the adsorption time is 120 minutes, the iodine adsorption capacity of the material rapidly rises to about 608 mg / g; the adsorption equilibrium is reached in about 180 minutes, and the highest adsorption capacity can reach 689.6 mg / g. The maximum adsorption amount of each sample was measured by four sets of parallel samples. As shown in Table 1, the average adsorption amount calculated by the data in the table is 636.7 mg / g, which is little difference from the adsorption kinetic curve of cuproxide aerogel material (difference <8%).

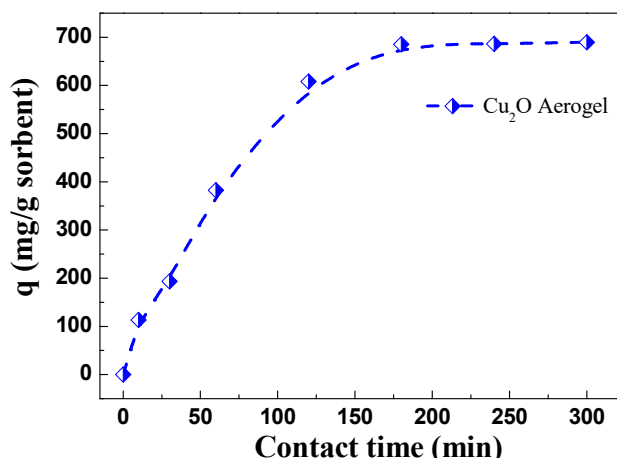


Figure 6. Kinetic curves for iodine adsorption by the Cu₂O aerogel at 75°C

Table 1. The maximum adsorption capacity of Cu₂O aerogel to I₂ in parallel experiments

Sample	Pre-adsorption weight m_1 (mg)	After adsorption weight m_2 (mg)	Adsorption capacity Q (mg/g)	Average adsorption capacity (mg/g)
1	203	326	605.9	636.7
2	202	328	623.8	
3	201	338	681.6	
4	203	332	635.5	

3.3 Adsorption Experiment of Iodine in Cyclohexane Solution

With cyclohexane as solvent of 1000 mg/l cyclohexane iodine solution as mother liquid, a certain quality of copper oxide aerogel adsorbent material, added to a certain initial concentration of

cyclohexane iodine solution, stirring at room temperature, iodine concentration in the filtrate is measured by ultraviolet spectrophotometer and record data, the capacity of copper oxide iodine adsorption can be calculated according to formula (7). In formula (7), q_e (mg/g) is the adsorption capacity, C_0 (mg/L) and C_e (mg/L) are the concentration of iodine in the solution before and after adsorption, V (L) is the initial volume of the solution, and M (g) is the adsorbent mass.

$$q_e = \frac{(C_0 - C_e)V}{M} \quad (7)$$

The kinetic adsorption experiment of iodine was completed at room temperature, where cyclohexane iodine solution volume (V) is 120 mL, iodine initial concentration (C_0) is 900 mg/L, cuprous oxide aerogel adsorbent mass (mg, and then the results of iodine adsorption experiment in cyclohexane were fitted according to pseudo-first-order kinetics model (8) and pseudo-second-order kinetics model (9). In formula (8)(9), q_t (mg/g) and q_e (mg/g) represent the adsorption amount of iodine at time t and equilibrium time, k_1 (min⁻¹) and k_2 g/(mg·min) indicate the primary adsorption rate constant and secondary adsorption rate constant respectively, and t (min) is the adsorption time.

$$\ln(q_e - q_t) = \ln q_e - k_1 t \quad (8)$$

$$\frac{t}{q_t} = \frac{1}{k_2 \times q_e^2} + \frac{t}{q_e} \quad (9)$$

According to the kinetic curve of iodine adsorption of copper oxide aerogel in cyclohexane solution (Figure 7), when the adsorption time is 0-60 minutes, the adsorption amount of iodine rises rapidly to about 122 mg/g; Cu₂O aerogel increases to about 137.7 mg/g for 90-210 minutes. Thereafter, the adsorption capacity remains stable in the adsorption process, the adsorption process is mainly stable chemical adsorption, and the delayed desorption produced by physical adsorption is rare, which has little impact on the adsorption properties of the material. According to the data in Table 2, the secondary adsorption kinetic model has a larger correlation coefficient r ($R^2 > 0.978$), which indicates that the adsorption process is more in line with the pseudo-second-order kinetics model, and the theoretical adsorption capacity of iodine in cyclohexane q_e is 159.7 mg/g.

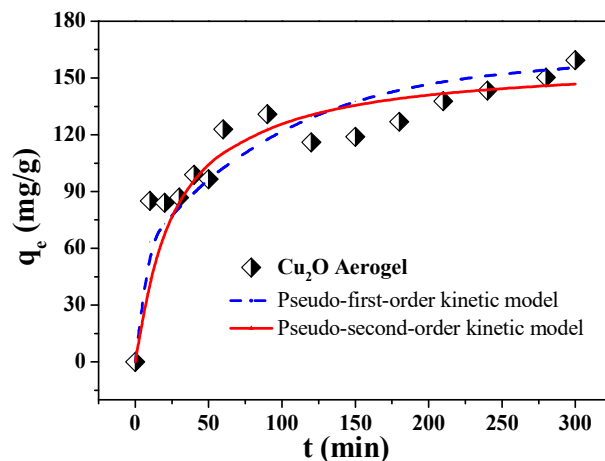


Figure 7. Kinetic fitting curve for iodine adsorption by a Cu₂O aerogel in a cyclohexane solution

Table 2. Fitting parameters of Cu₂O aerogel to I₂ kinetics adsorption model

	pseudo-first-order kinetics			pseudo-second-order kinetics		
q _t (mg/g)	k ₁	q _e (mg/g)	R ²	k ₂	q _e (mg/g)	R ²
159.40	0.01	107.38	0.647	2.4×10 ⁻⁴	159.74	0.978

3.4 Isothermal Adsorption

At room temperature (25°C), cyclohexane iodine solution (initial concentration C₀ = 50 mg/L, 100 mg/L, 200 mg/L, 300 mg/L, 500 mg/L, 800 mg/L, 1000 mg/L) and the data were fitted according to Langmuir equation (10) and Freundlich equation (11), as shown in Figure 8.

$$\frac{C_e}{q_e} = \frac{C_e}{q_{max}} + \frac{1}{bq_{max}} \tag{10}$$

$$\ln q_e = \ln K_f + n \ln C_e \tag{11}$$

In formula (10)(11), C_e (mg/L) and q_e (mg/g) are the iodine content adsorbed per unit weight of the adsorbent and the concentration of iodine in the solution at equilibrium, respectively. The K_f (mg/g) represents the adsorption capacity of the multilayers, and n is an empirical parameter related to the adsorption strength. The K_f and n are determined by the intercept and slope of the linear plots of lnq_e and lnC_e, respectively. The b (l/mg) is the Langmuir constant associated with the adsorption free energy. The q_{max} is the monolayer absorption capacity of the sorbent. The q_{max} and b are calculated from the slope and intercept of the linear plots of C_e /q_e and C_e, respectively.

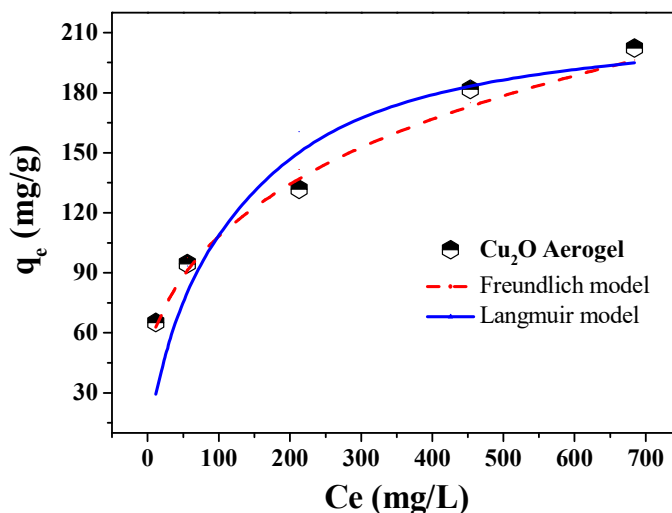


Figure 8. Isothermal adsorption curves of I₂ by a Cu₂O aerogel in a cyclohexane solution

From Table 3, the correlation coefficient as described for the Langmuir model and Freundlich model fit is very close (R²> 0.971 and R²> 0.985), it shows that the adsorption process of iodine by cuprous oxide aerogel complies with the description of the Langmuir model and Freundlich model, it shows that this adsorption process is coordinated by chemical and physical adsorption[15], the good adsorption stability is similar to the results of the previous adsorption kinetic analysis, It also shows that the distribution of adsorption sites for iodine affinity on the surface of cuprous oxide aerogel is

relatively uniform, the results of the fit showed that, the theoretical adsorption capacity of iodine by the cuprous oxide aerogel material in cyclohexane is 215.9 mg/g.

Table 3. Fitting parameters of isothermal adsorption curves for Cu₂O aerogel adsorption I2

Langmuir constant			Freundlich constant		
q _m (mg/g)	K _L (L/mg)	R ²	n	K _F (mg/g)	R ²
215.98	0.013	0.971	0.279	31.67	0.985

4. Conclusion

Cu₂O aerogel material is successfully prepared by sol-gel method. Series characterization of the Cu₂O aerogel material shows that Cu₂O nanorods are self-assembled into a three-dimensional network porous structure with a specific surface area of 2.1 m²/g and a pore size distribution of 3-18 nm, as typical structural characteristics of the aerogel material. The porous structure in the Cu₂O aerogel can effectively promote the rapid enrichment of iodine. Through the adsorption experiments of vapor and cyclohexane solutions, the adsorption behavior of iodine on Cu₂O aerogel was systematically investigated, the iodine adsorption kinetics of Cu₂O aerogels were found to fit the description of Pseudo-second-order kinetics model, and isothermal adsorption as described by both Langmuir model and Freundlich model, it shows that its adsorption of iodine is the joint effect of chemical adsorption and physical adsorption, the maximum adsorption capacity for iodine adsorption is 636.7 mg/g and the sorption process reached equilibrium within 180 min, show the good adsorption properties of gaseous iodine. Furthermore, Cu₂O aerogel exhibited low-cost preparation, excellent adsorption performance and good stability which was suitable for real applications in the nuclear industry.

Acknowledgments

This work was supported by Sichuan Innovation and Entrepreneurship Training Program For College students (21XC029).

References

- [1] S.U. Nandanwar, K. Coldsnow, V. Utgikar, P. Sabharwall, D.E. Aston, D. Eric Aston, Capture of harmful radioactive contaminants from off-gas stream using porous solid sorbents for clean environment – a review[J]. Chem. Eng. J. 306 (2016) :369–381.
- [2] B.J. Riley, J.D. Vienna, D.M. Strachan, J.S. McCloy, J.L. Jerden, Materials and processes for the effective capture and immobilization of radioiodine: a review[J]. J. Nucl. Mater. 470 (2016):307–326.
- [3] M.I. Ojovan, W.E. Lee, Glassy wastefoms for nuclear waste immobilization[J]. Metall. Mater. Trans. A Phys. Metall. Mater. Sci. 42 (2011): 837–851.
- [4] Rohde, R.A.; Muller, R.A. Air Pollution in China: Mapping of Concentrations and Sources[J]. PLoS ONE 2015, 10, e0135749.
- [5] Jia, Y.; Gao, Y.; Xu, Z.; Wong, K.P.; Lai, L.L.; Xue, Y.; Dong, Z.Y.; Hill, D.J. Powering China's sustainable development with renewable energies: Current status and future trend[J]. Electr. Power Compon. Syst. 2015, 43, 1193–1204.
- [6] C.C. Lin, Volatility of iodine in dilute aqueous solutions[J]. J. Inorg. Nucl. Chem. 43 (1981):3229–3238.
- [7] E.A. Pillar, M.I. Guzman, J.M. Rodriguez, Conversion of iodide to hypoiodous acid and iodine in aqueous microdroplets exposed to ozone[J]. Environ. Sci. Technol. 47 (2013):10971–10979.
- [8] Guo, X.; Guo, X. Nuclear power development in China after the restart of new nuclear construction and approval: A system dynamics analysis[J]. Renew. Sustain. Energy Rev. 2016, 57, 999–1007.

- [9] Oscarson, D.W.; Miller, H.G.; Watson, R.L. The potential effectiveness of mercury minerals in decreasing the level of iodine-129 in a nuclear fuel waste disposal vault[J]. Nucl. Chem. Waste Manag. 1986, (6): 151–157.
- [10] Banerjee D, Chen X, Lobanov S, et al. Iodine adsorption in metal organic frameworks in the presence of humidity[J]. ACS Applied Materials & Interfaces, 2018, 10(13): 10622–10626.
- [11] Yu F, Chen Y, Wang Y, et al. Enhanced removal of iodide from aqueous solution by ozonation and subsequent adsorption on Ag-Ag₂O modified on carbon spheres[J]. Applied Surface Science, 2018, 427: 753–762.
- [12] Kitada S, Oikawa T, Watanabe S, et al. Removal of radioactive iodine and cesium in water purification [J]. Desalination & Water Treatment, 2014, 27(12): 1–8.
- [13] Sekizawa J. Risk communication about radionuclide contamination of food after the Fukushima nuclear power plant accident[J]. Shokuhinseigaku Zasshi Journal of the Food Hygienic Society of Japan, 2013, 54(2): 89.
- [14] Sigen A, Zhang Y, Li Z, et al. Highly efficient and reversible iodine capture using a metalloporphyrin-based conjugated microporous polymer[J]. Chemical Communications, 2014, 50(62): 8495–8498.
- [15] B.J. Riley, J D. Vienna, D M Strachan, et al. Materials and processes for the effective capture and immobilization of radioiodine: A review[J]. Journal of Nuclear Materials 2016,(470):307e326.
- [16] Inoue, H. Effects of co-ions on transport of iodide ions through a non-conventional anion exchange paper membrane[J]. J. Membr. Sci. 2004, 228, 209–215.
- [17] Liu, L.; Liu, W.; Zhao, X.; Chen, D.; Cai, R.; Yang, W.; Komarneni, S.; Yang, D. Selective capture of iodide from solutions by microrosette-like δ -Bi₂O₃[J]. ACS Appl. Mater. Interfaces 2014, 6, 16082–16090.
- [18] K.W. Chapman, P.J. Chupas, T.M. Nenoff. Radioactive iodine capture in silver-containing mordenites through nanoscale silver iodide formation[J]. J. Am. Chem. Soc. 2010, (132):8897–8899.
- [19] Eldar P. Magomedbekov, Alexander V. Obruchikov. A method for properties evaluation of activated charcoal sorbents in iodine capture under dynamic conditions[J]. Nuclear Engineering and Technology, 2019, (51):641-645.
- [20] Mao, P.; Qi, B.; Liu, Chen, S, et al. Ag(II) doped MIL-101 and its adsorption of iodine with high speed in solution[J]. J. Solid State Chem. 2016, (237):274–283.
- [21] Ping Wang, Qing Xu, Donglin Jiang. Exceptional Iodine Capture in 2D Covalent Organic Frameworks[J]. Adv. Mater. 2018, (30): 1801991(1-7).
- [22] Geng T M , Liu M , Chen H, et al. Flexible Oxygen-Bridged Porous Organic Polymers for Adsorbing and Fluorescence Sensing Iodine and the Formation of Liquid Complexes of POPs-(Poly)Iodide Anions[J]. Macromol. Mater. Eng. 2021, (306):2000711.
- [23] K. S. Subrahmanyam, Brian J. Riley, Mercuri G. Kanatzidis, et al. Chalcogenide Aerogels as Sorbents for Radioactive Iodine[J]. Chem. Mater. 2015, 27, 2619-2626.
- [24] B J Riley, J O Kroll, J A Peterson, et al. Silver-Loaded Aluminosilicate Aerogels As Iodine Sorbents[J]. ACS Appl. Mater. Interfaces, 2017, 9, 38, 32907–32919.
- [25] K S Subrahmanyam, D Sarma, M G Kanatzidis, et al. Chalcogenide Aerogels as Sorbents for Radioactive Iodine[J]. Chem Mater. 2015, 27, 2619-2626.
- [26] Xiong Y, Dang B K, Sun Q f , et al. Cellulose Fibers Constructed Convenient Recyclable 3D Graphene-Formicary-like-Bi₂O₃ Aerogels for the Selective Capture of Iodide[J]. ACS Appl. Mater. Interfaces 2017, 9, 24, 20554–20560.
- [27] Mao, P.; Qi, L.; Liu, X.; Liu, Y.; Jiao, Y.; Chen, S.; Yang, Y. Synthesis of Cu/Cu₂O hydrides for enhanced removal of iodide from water[J]. Hazard. Mater. 2017, 328, 21–28.
- [28] Gao, S.; Yang, J.; Li, Z.; Jia, X.; Chen, Y. Bioinspired synthesis of hierarchically micro/nano-structured CuI tetrahedron and its potential application as adsorbent for Cd(II) with high removal capacity. J. Hazard. Mater. 2012, 211, 55–61.
- [29] Yang S, Zhang S, Peng F, et al. Facile synthesis of self-assembled mesoporous CuO nanospheres and hollow Cu₂O microspheres with excellent adsorption performance[J]. RSC Adv. 2014, (4): 43024–43028.

- [30] Li W Y, Gong S, Cheng W L, et al. Soft piezoresistive pressure sensing matrix from copper nanowires composite aerogel[J]. *Science Bulletin*, 2016, 61, 20: 1624-1630.
- [31] Mohamed, R.M.; Aazam, E.S. Preparation and characterization of core-shell polyaniline/mesoporous Cu₂O nanocomposites for the photocatalytic oxidation of thiophene. *Appl. Catal. A* 2014, 480, 100–107.